

Observation of an Electric Quadrupole Transition in a Negative Ion: Experiment and Theory

C. W. Walter¹, S. E. Spielman¹, R. Ponce¹, and N. D. Gibson¹

Department of Physics and Astronomy, Denison University, Granville, Ohio 43023, USA

J. N. Yukich²

Physics Department, Davidson College, Davidson, North Carolina 28035, USA

C. Cheung³

Department of Physics and Astronomy, University of Delaware, Newark, Delaware 19716, USA

M. S. Saffronova

Department of Physics and Astronomy, University of Delaware, Newark, Delaware 19716, USA

Joint Quantum Institute, National Institute of Standards and Technology and the University of Maryland, College Park, Maryland 20742, USA



(Received 20 November 2020; accepted 15 January 2021; published 26 February 2021)

The first direct experimental observation of an electric quadrupole ($E2$) absorption transition between bound states of an atomic negative ion has been made. The transition was observed in the negative ion of bismuth by resonant ($1 + 1$) photon detachment from Bi^- via ${}^3P_2 \rightarrow {}^3P_0$ excitation. The $E2$ transition properties were completely independently calculated using a hybrid theoretical approach to account for the strong multilevel electron interactions and relativistic effects. The experimental and *ab initio* theoretical results are in excellent agreement, providing valuable new insight into this complex system and forbidden transitions in negative ions more generally.

DOI: 10.1103/PhysRevLett.126.083001

Although optical transitions between bound states of both neutral atoms and positive ions have been extensively studied for more than a century, similar transitions between bound states of *negative* ions have only been observed much more recently [1]. This difference in discovery date is due, in part, to the fundamental nature of negative ions: In sharp contrast to the infinite number of bound states in atoms and positive ions, since negative ions are not held together by a net Coulomb potential, their short-range polarization potentials can support only one or at most a few bound states [2,3] making possible transitions very scarce.

The first observation of a bound-bound electric dipole ($E1$) transition in an atomic negative ion was reported only 20 years ago (in Os^-) [4], and magnetic dipole ($M1$) transitions in negative ions in the optical regime had been first observed just 4 years earlier (in Ir^- and Pt^-) [5,6]. Since these initial discoveries, $E1$ transitions have been observed in very few other negative ions (e.g., Ce^- [7] and La^- [8]), and $M1$ transitions have been observed in several additional negative ions [9,10]. However, previous experimental searches for electric quadrupole ($E2$) transitions in negative ions have not succeeded, due to the very small transition rates and large background signals from continuum photodetachment [5,10]. In the

present work, we report the first direct experimental observation of an $E2$ absorption transition between bound states of an atomic negative ion (Bi^-), together with high-precision *ab initio* theoretical calculations of the energy and rate of the transition.

Electric quadrupole atomic transitions are of great interest due to applications including tests of fundamental physics [11–13], optical clocks [14], and quantum information [15], and they provide important benchmarks for detailed state-of-the-art theoretical calculations [16]. The properties of negative ions crucially depend on electron correlation effects [1–3,17–19], and $E2$ transitions in negative ions provide uniquely valuable opportunities to gain insight into these subtle but important interactions. Accurate theoretical computations are very difficult for negative ions with complex electronic structure due to large configuration mixing in comparison with neutrals or positive ions [1,17].

There is even greater urgency for studying forbidden transitions in negative ions with the advent of new cryogenic storage ring facilities, such as DESIREE [20,21] and the CSR [22,23], that can measure lifetimes of excited states of negative ions over unprecedentedly long scales of hours [21]. While most of the negative ion excited state lifetime experiments to date have involved $M1$ transitions, one recent

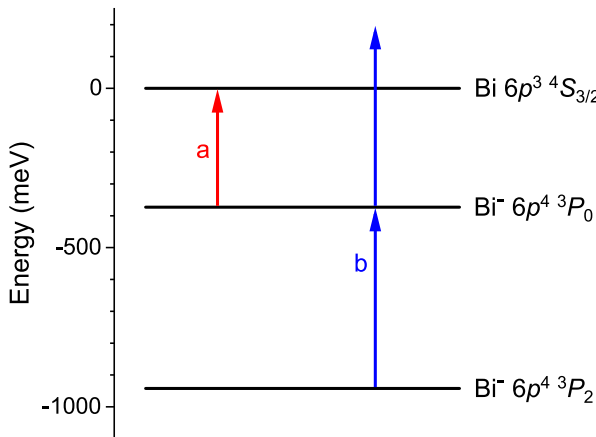


FIG. 1. Energy levels for the two bound states of Bi^- and the ground state of Bi with arrows showing the two measurements performed: (a, red) single-photon threshold detachment from $\text{Bi}^- {}^3P_0$ and (b, blue) resonant $(1+1)$ photon detachment via the $\text{Bi}^- {}^3P_2 \rightarrow {}^3P_0$ E2 transition.

study at DESIREE measured the E2 decay of an excited state of Pt^- [24].

The present work investigates an E2 transition in the negative ion of bismuth both experimentally and theoretically. The hyperfine-averaged binding energy of the $\text{Bi}^- (6p^4 {}^3P_2)$ ground state relative to the Bi $(6p^3 {}^4S_{3/2})$ ground state was previously measured by Bilodeau and Haugen to be 942.369(13) meV [25]. While the Bi^- fine structure has not been previously measured, Su *et al.* recently reported calculations indicating an inverted energy ordering of the excited fine structure levels, with 3P_0 being bound and 3P_1 unbound [26].

We performed two complementary experiments in the present work (see Fig. 1): (1) measurement of the binding energy of the $\text{Bi}^- {}^3P_0$ excited state using photodetachment threshold spectroscopy and (2) observation of the $\text{Bi}^- {}^3P_2 \rightarrow {}^3P_0$ transition via resonant $(1+1)$ photon detachment. The observed resonance transition has $|\Delta J| = 2$; therefore, it is strictly forbidden for E1 or M1 processes, and it must proceed by the E2 interaction. Although there have been previous observations of transitions in negative ions that had both M1 and E2 contributions [9,10], to our knowledge, this is the first absorption transition observed in a negative ion with E2 as the lowest-order allowed interaction. The Bi^- fine structure and E2 transition properties were completely independently calculated without foreknowledge of the present experimental values using a high-precision hybrid theoretical approach to account for the strong multilevel electron interactions and relativistic effects. The experimental and theoretical results are in excellent agreement, providing valuable new insight into this complex system and testing the accuracy of the theoretical approach.

Photodetachment from Bi^- was measured as a function of photon energy using a crossed ion-beam-laser-beam

system described previously [7,27]. Negative ions produced by a cesium sputter source [28] using a cathode packed with bismuth powder were accelerated to 12 keV and magnetically mass selected producing ~ 1 nA of ${}^{209}\text{Bi}^-$ (the only long-lived naturally occurring isotope). The ion beam was intersected perpendicularly by a pulsed laser beam, following which residual negative ions were electrostatically deflected into a Faraday cup, while neutral atoms produced by photodetachment continued undeflected to a multidynode detector. The neutral atom signal was normalized to the ion-beam current and the photon flux measured for each laser pulse. The spectra were obtained by repeatedly scanning the laser wavelength and then sorting the data into photon energy bins of selectable width.

The laser system was an optical parametric oscillator and amplifier (LaserVision) pumped by a 20-Hz Nd:YAG laser, giving an operating range of 5000–1300 nm (250–920 meV) with bandwidth ~ 0.01 meV. Long focal length lenses approximately collimated the beam. For the E2 transition measurement, an additional 50-cm focal length lens about 40 cm from the interaction region increased the intensity to drive this very weak transition. Note that hyperfine (hf) structure is not resolvable in the present experiments, since the laser bandwidth is on the order of or larger than the hf splittings of Bi ${}^4S_{3/2}$ (nuclear spin 9/2 giving four hf levels with measured intervals < 0.012 meV [29]), $\text{Bi}^- {}^3P_2$ (five hf levels with calculated intervals < 0.005 meV [30]), and $\text{Bi}^- {}^3P_0$ (no hf structure since $J = 0$). Therefore, the measured threshold and transition energies are reported as hf-averaged values.

The Bi^- photodetachment spectrum was measured over 255–920 meV, revealing only a single threshold near 373 meV, which is due to detachment from the $\text{Bi}^- {}^3P_0$ excited state to the $\text{Bi} {}^4S_{3/2}$ ground state. Figure 2 shows the neutral atom signal near the observed threshold. Note that most of the ions in the beam are in the 3P_2 ground state rather than the 3P_0 excited state. Relative photodetachment signal rates 0.5 meV above threshold in the present experiment compared to our recent measurements of Ti^- [31] indicate that $\text{Bi}^- {}^3P_0$ makes up only $\sim 0.3\%$ of the beam, consistent with estimates based on a Boltzmann statistical distribution at the approximate ion source temperature of ~ 1500 K. Also, there is a small background signal below the 3P_0 threshold; since no more weakly bound states of Bi^- are expected, this background is likely due to a slight leakage of the optical parametric oscillator “signal” light at a photon energy of 1.96 eV which is sufficient to photodetach the large population of ground state Bi^- ions in the beam.

The threshold energy for $\text{Bi}^- (6p^4 {}^3P_0)$ detachment can be precisely determined from the data in Fig. 2 using the Wigner threshold law [32]. In the present case, a p electron is detached, so the cross section closely above threshold is dominated by s -wave detachment and increases as

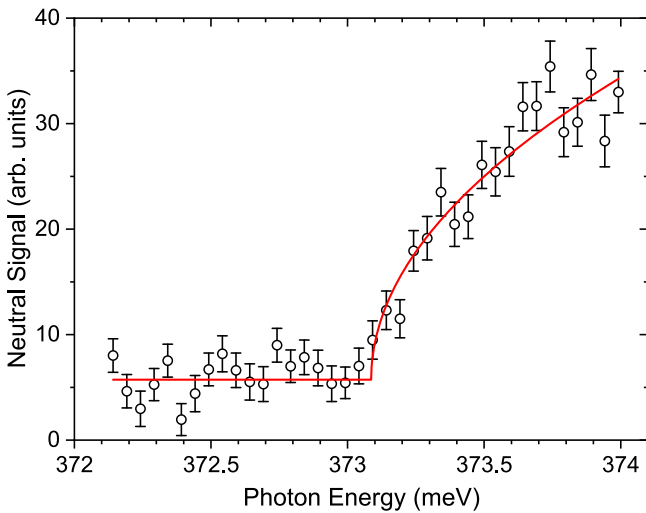


FIG. 2. Measured photodetachment threshold from the $\text{Bi}^- {}^3P_0$ excited state to the $\text{Bi} {}^4S_{3/2}$ ground state: circles, data; line, s -wave Wigner law fit.

$(E - E_t)^{1/2}$, where E is the photon energy and E_t is the threshold energy. The Wigner law provides an excellent fit to the data, yielding the detachment threshold corresponding to the binding energy of $\text{Bi}^- {}^3P_0$ to be 373.09(4) meV.

After establishing the binding energy of the excited state, we searched for and found the $\text{Bi}^- {}^3P_2 \rightarrow {}^3P_0$ electric quadrupole transition. The expected transition energy of 569.28(4) meV is given by the difference between the hf-averaged binding energies of the $\text{Bi}^- {}^3P_2$ ground state [942.369(13) meV [25]] and the $\text{Bi}^- {}^3P_0$ excited state [373.09(4) meV]. Figure 3 shows the neutral atom signal measured near the expected transition; a peak in the signal is visible due to resonant $(1 + 1)$ photodetachment from $\text{Bi}^- {}^3P_2$ via $E2$ excitation of $\text{Bi}^- {}^3P_0$ followed by absorption of a second photon to detach the excited state. Observation of this resonance transition in the present experiment was possible in part because the single-photon detachment background signal is low due to the small fraction of excited state ions in the beam. A Lorentzian fit to the measured data yields the transition energy to be 569.27(3) meV, in excellent agreement with the expected value of 569.28(4) meV based on the difference in binding energies. The fitted peak width of 0.023(5) meV is an upper limit rather than the natural width of the transition, because of broadening by the laser bandwidth and unresolved hf structure.

The measurements reported in this work provide an excellent opportunity to test the accuracy of theory in this complicated negative ion. We carried out calculations of the Bi^- binding energies and the ${}^3P_2 \rightarrow {}^3P_0$ transition energy and rate using a hybrid approach that combines the configuration interaction (CI) and the coupled-cluster method (CI + all-order method) [33]. This method allows efficient inclusion of both strong valence-valence

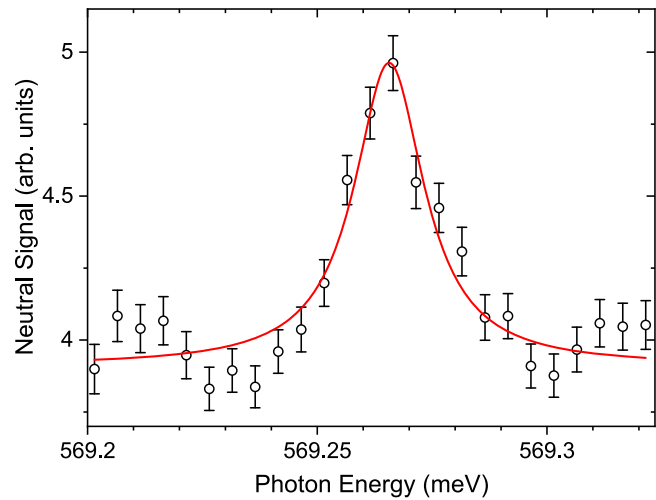


FIG. 3. Measured peak for resonant $(1 + 1)$ photodetachment via the $\text{Bi}^- {}^3P_2 \rightarrow {}^3P_0$ $E2$ transition: circles, data; line, Lorentzian fit.

correlations (via the CI) and core excitations from the entire core (by the coupled-cluster approach). The many-electron wave function is obtained as usual in the framework of the CI method, but the energies and wave functions of the low-lying states are determined by diagonalizing the effective (rather than bare CI) Hamiltonian. It is constructed using a combination of the coupled-cluster approach that allows single and double excitation from the entire core and the many-body perturbation theory (MBPT). Alternatively, we carried out identical computations constructing the entire effective Hamiltonian using the second-order MBPT [34] to evaluate the importance of the higher-order (HO) corrections; we refer to such results as the CI + MBPT.

We treat Bi as a system with 3 valence electrons and a $[\text{Xe}]4f^{14}5d^{10}6s^2$ core. The core is the same for the Bi^- calculation. The difference between the Bi^- and Bi calculation is in the CI part, which contains 4 valence electrons for Bi^- . There is an exponential growth in the number of possible configurations with the addition of extra valence electrons and care must be taken to ensure a sufficiently large set of configurations for Bi^- . The problem is exacerbated for the weakly bound negative ion which exhibits very strong configuration mixing. We carried out a number of tests to demonstrate the convergence of the results with an increasing number of configurations, with structured multistep expansion of the configuration sets using prior runs to establish the important configurations; see Supplemental Material for details of these tests [35]. All calculations incorporate the Breit interaction as described in Ref. [36].

The results of the CI + all-order and CI + MBPT calculations and specific contributions to the energies are summarized for Bi^- in Table I; see Supplemental Material for Bi results [35]. Binding energies are shown relative to the $\text{Bi} 6p^3 {}^4S_{3/2}$ ground state. Contributions of the higher

TABLE I. Calculated binding energies of Bi^- bound states relative to the $\text{Bi}^4S_{3/2}$ ground state and transition energy for $\text{Bi}^- {}^3P_2 \rightarrow {}^3P_0$ compared to experimental measurements in meV. Contributions of the higher orders (HO) are calculated as the differences of the CI + all-order (CI + all) and CI + MBPT calculations. QED corrections and contributions of the higher partial wave ($l = 6$) are listed separately. “Extra conf.” lists the difference of the results of the large and medium CI calculations. “Final” results were obtained by including all of these corrections in the same computation. “Diff.” and “Diff.%” are the difference between the experimental and final calculated energies.

	J	Experiment	CI + MBPT	CI + all	HO	$l = 6$	QED	Extra conf.	Final	Diff.	Diff.%	
Bi^-	$6p^4 {}^3P$	2	942.369(13) ^a	910.4	911.0	0.6	2.1	2.1	26.7	941.9	0.5	0.05%
	$6p^4 {}^3P$	0	373.09(4) ^b	321.2	342.6	21.3	1.0	1.4	26.0	371.0	2.1	0.6%
	${}^3P_2 \rightarrow {}^3P_0$		569.27(3) ^b	589.2	568.5	-20.7	1.1	0.7	0.6	570.9	-1.7	0.3%

^aReference [25], hyperfine averaged.

^bPresent measurements.

orders are calculated as the differences of the CI + all-order and CI + MBPT calculations. To evaluate the accuracy of the calculations, we calculated several smaller corrections separately. We originally ran CI + all-order and CI + MBPT calculations allowing excitations to all partial waves up to $l = 5$, with maximum principal quantum number $n = 35$ for each (relativistic) partial wave. The contribution of the $l = 6$ partial wave is listed in the column “ $l = 6$ ” in Table I. From the extrapolations carried out for simpler systems, we find that the contribution of all other partial waves is on the same order as the $l = 6$ contribution. QED corrections were calculated following Ref. [37]. Both of these corrections are relatively small. Next, we increase the number of CI configurations allowing excitations up to $23spdf18g$ and $22spdf18g$ orbitals for Bi and Bi^- , respectively, an increase from the initial $22spd18f14g$ set. All single, all double, and a large subset of triple excitations are included. These changes increase the number of included configurations for Bi^- from 73 719 to 126 168, with corresponding increase in the number of Slater determinants from 3 090 923 to 4 952 692. Finally, we carried out a complete CI + all-order run that incorporated all corrections (QED, $l = 6$, and larger number of configurations) simultaneously. These results are listed as “Final” in Table I.

Our final calculated binding energy of the $\text{Bi}^- {}^3P_2$ ground state is in excellent agreement with the measured value of Bilodeau and Haugen [25], differing by only 0.5 meV (0.05%) (see Table I). We find that the binding energy of the ground state is strongly affected by the inclusion of more configurations but not by the inclusion of the higher orders. This is expected since the Bi and Bi^- computations share the same core; thus, difference in its treatment is expected to cancel to a degree. A sensitivity to extra configurations is also expected as configuration mixing for Bi^- is much stronger than for Bi. There is also excellent agreement for the binding energy of the fine structure excited state 3P_0 , with our calculation of 371.0 meV being within 2.1 meV (0.6%) of our measurement of 373.09(4) meV. However, in contrast to the ground

state, higher orders contribute significantly (5.7%) to the binding energy of the 3P_0 state and therefore affect the ${}^3P_2 \rightarrow {}^3P_0$ transition energy. Also, our calculations indicate that the $\text{Bi}^- {}^3P_1$ state is not bound, in agreement with the calculations of Su *et al.* [26].

It is interesting to also explore if Po, which is isoelectronic to Bi^- , may be used as a homologue system to improve prediction for the negative ion. We carried out a Po computation with all parameters identical to Bi^- [35]. As for Bi^- , Po shows an inverted energy ordering of fine structure levels ($J = 2, 0, 1$) [38], illustrating a similarity between the neutral and negative ion systems. However, we find that the difference between our calculations and the experimental energies is actually larger in Po than in Bi^- . Most likely, this is due to uneven cancellation of some omitted effects, such as core triple excitations and nonlinear terms that tend to strongly cancel. We also find as expected that there is much stronger configuration mixing in the negative ion; for example, only 11 nonrelativistic configurations contribute a total of 99% for the ground state of Po, but 22 configurations are needed for Bi^- . Our results demonstrate the significant fact that an isoelectronic neutral system cannot always be used as a homologue for a negative ion.

The present experimental and theoretical results for the $\text{Bi}^- {}^3P_2 \rightarrow {}^3P_0$ E2 transition are given in Table II, together with previous calculations. Our calculated transition energy (570.9 meV) is in excellent agreement with our experimental value [569.27(3) meV], differing by only 1.7 meV

TABLE II. Present results and previous calculations for the $\text{Bi}^- {}^3P_2 \rightarrow {}^3P_0$ E2 transition energy and upper-state lifetime.

Study	Method	${}^3P_2 \rightarrow {}^3P_0$ Energy (meV)	Lifetime (s)
Present	Experiment	569.27(3)	
Present	Theory	570.9	16.5(7)
Su <i>et al.</i> [26]	Theory	624.0	15.20
Konan <i>et al.</i> [39]	Theory	1100.0	

(0.3%). In contrast, the calculated transition energy from Su *et al.* [26] is 54.7 meV larger than our measurement, while the earlier calculation of Konan *et al.* [39] is even farther away. Our computations include higher-order inner-shell electronic correlations and, therefore, are expected to be more accurate than multiconfiguration Dirac-Hartree-Fock calculations [26,39] for both energies and transition rates.

For the transition rate, we calculate the electric quadrupole $6p^4 \ ^3P_2 - ^3P_0$ reduced matrix element to be $16.30(33)ea_0^2$ using the CI + all-order method. There is only a 1% difference between the CI + all-order and the CI + MBPT results, and there is a 1.7% difference between the results obtained with medium and large sets of CI configurations. We add these in quadrature to estimate the final uncertainty of the matrix element to be 2%. Using the experimental value of the transition energy, we obtain $0.0607(24) \text{ s}^{-1}$ for the transition rate, corresponding to a 3P_0 lifetime of $16.5(7) \text{ s}$. At first glance, the previous calculated lifetime by Su *et al.* [26] of 15.20 s appears to be fairly close to our value. However, it is important to consider that the quoted lifetime of Su *et al.* was obtained using their calculated transition energy for $^3P_2 \rightarrow ^3P_0$, which is larger than our precisely measured energy by $\sim 10\%$. Since the $E2$ lifetime scales inversely with transition energy to the fifth power, revising their lifetime using our measured energy would yield an adjusted lifetime of 24.05 s , which is significantly longer than our value. Finally, note that although our calculated lifetime of the 3P_0 upper state of $16.5(7) \text{ s}$ indicates that the transition is far too narrow ($\sim 4 \times 10^{-14} \text{ meV}$) for a measurement of the lifetime from the peak width in the present experiment, the theoretically predicted lifetime could be rigorously tested in storage ring experiments using established methods [21,24].

In summary, we have measured the binding energy of the $\text{Bi}^- \ ^3P_0$ excited state and observed its excitation from the $\text{Bi}^- \ ^3P_2$ ground state using resonant $(1+1)$ photodetachment. To our knowledge, this is the first direct observation of an $E2$ absorption transition between bound states of an atomic negative ion. Furthermore, we have confirmed the Bi^- fine structure and the $E2$ character of the transition through *ab initio* theoretical calculations including the transition rate. The measured and calculated energies are in excellent agreement, demonstrating the power of the theoretical methods used to account for the important correlation and relativistic effects in this complex multi-electron system.

Similar experimental and theoretical methods can be applied to study $E2$ transitions in other negative ions that have appropriate excited bound state structures, opening a new avenue for investigations of forbidden transitions in atomic systems. Such studies can be combined with the new ability to accurately measure lifetimes of excited negative ions over long timescales recently developed at cryogenic storage ring facilities such as DESIREE and the

CSR to give further insight into many-body correlation effects and decay dynamics.

We thank Charles W. Clark for insightful discussions. This work was supported in part by U.S. NSF Grants No. PHY-1620687 and No. PHY-1707743. This research was performed in part under the sponsorship of the U.S. Department of Commerce, National Institute of Standards and Technology. The theoretical research was supported in part through the use of Information Technologies resources at the University of Delaware, specifically the high-performance Caviness computing cluster.

- [1] T. Andersen, *Phys. Rep.* **394**, 157 (2004).
- [2] T. Andersen, H. K. Haugen, and H. Hotop, *J. Phys. Chem. Ref. Data* **28**, 1511 (1999).
- [3] D. J. Pegg, *Rep. Prog. Phys.* **67**, 857 (2004).
- [4] R. C. Bilodeau and H. K. Haugen, *Phys. Rev. Lett.* **85**, 534 (2000).
- [5] J. Thøgersen, M. Scheer, L. D. Steele, H. K. Haugen, and W. P. Wijesundara, *Phys. Rev. Lett.* **76**, 2870 (1996).
- [6] Radio frequency spectroscopy had previously been applied to $M1$ transitions in the helium negative ion; D. L. Mader and R. Novick, *Phys. Rev. Lett.* **29**, 199 (1972).
- [7] C. W. Walter, N. D. Gibson, Y.-G Li, D. J. Matyas, R. M. Alton, S. E. Lou, R. L. Field III, D. Hanstorp, L. Pan, and D. R. Beck, *Phys. Rev. A* **84**, 032514 (2011).
- [8] C. W. Walter, N. D. Gibson, D. J. Matyas, C. Crocker, K. A. Dungan, B. R. Matola, and J. Rohlén, *Phys. Rev. Lett.* **113**, 063001 (2014).
- [9] M. Scheer, H. K. Haugen, and D. R. Beck, *Phys. Rev. Lett.* **79**, 4104 (1997).
- [10] M. Scheer, R. C. Bilodeau, C. A. Brodie, and H. K. Haugen, *Phys. Rev. A* **58**, 2844 (1998).
- [11] J. C. Berengut, V. A. Dzuba, and V. V. Flambaum, *Phys. Rev. Lett.* **105**, 120801 (2010).
- [12] V. A. Dzuba, M. S. Safronova, U. I. Safronova, and V. V. Flambaum, *Phys. Rev. A* **92**, 060502(R) (2015).
- [13] C. Sanner, N. Huntemann, R. Lange, C. Tamm, E. Peik, M. S. Safronova, and S. G. Porsev, *Nature (London)* **567**, 204 (2019).
- [14] A. D. Ludlow, M. M. Boyd, J. Ye, E. Peik, and P. O. Schmidt, *Rev. Mod. Phys.* **87**, 637 (2015).
- [15] P. Schindler, D. Nigg, T. Monz, J. T. Barreiro, E. Martinez, S. X. Wang, S. Quint, M. F. Brandl, V. Nebendahl, C. F. Roos, M. Chwalla, M. Hennrich, and R. Blatt, *New J. Phys.* **15**, 123012 (2013).
- [16] U. I. Safronova, M. S. Safronova, and W. R. Johnson, *Phys. Rev. A* **95**, 042507 (2017).
- [17] C. F. Fischer, *Phys. Scr.* **40**, 25 (1989).
- [18] V. K. Ivanov, *Radiat. Phys. Chem.* **70**, 345 (2004).
- [19] M. T. Eiles and C. H. Greene, *Phys. Rev. Lett.* **121**, 133401 (2018).
- [20] R. D. Thomas *et al.*, *Rev. Sci. Instrum.* **82**, 065112 (2011).
- [21] E. Bäckström, D. Hanstorp, O. M. Hole, M. Kaminska, R. F. Nascimento, M. Blom, M. Björkhage, A. Källberg, P. Löfgren, P. Reinhard, S. Rosén, A. Simonsson,

R. D. Thomas, S. Mannervik, H. T. Schmidt, and H. Cederquist, *Phys. Rev. Lett.* **114**, 143003 (2015).

[22] R. von Hahn *et al.*, *Rev. Sci. Instrum.* **87**, 063115 (2016).

[23] C. Meyer *et al.*, *Phys. Rev. Lett.* **119**, 023202 (2017).

[24] K. C. Chartkunchand *et al.*, *Phys. Rev. A* **94**, 032501 (2016).

[25] R. C. Bilodeau and H. K. Haugen, *Phys. Rev. A* **64**, 024501 (2001).

[26] Y. Su, R. Si, K. Yao, and T. Brage, *J. Phys. B* **52**, 125002 (2019).

[27] C. W. Walter, N. D. Gibson, D. J. Carman, Y.-G Li, and D. J. Matyas, *Phys. Rev. A* **82**, 032507 (2010).

[28] R. Middleton, *A Negative-Ion Cookbook* (University of Pennsylvania, Philadelphia, PA, 1990).

[29] R. J. Hull and O. Brink, *Phys. Rev. A* **1**, 685 (1970).

[30] D. R. Beck (unpublished); see Ref. [25].

[31] C. W. Walter, N. D. Gibson, and S. E. Spielman, *Phys. Rev. A* **101**, 052511 (2020).

[32] E. P. Wigner, *Phys. Rev.* **73**, 1002 (1948).

[33] M. S. Safronova, M. G. Kozlov, W. R. Johnson, and D. Jiang, *Phys. Rev. A* **80**, 012516 (2009).

[34] M. G. Kozlov, S. G. Porsev, M. S. Safronova, and I. I. Tupitsyn, *Comput. Phys. Commun.* **195**, 199 (2015).

[35] See Supplemental Material at <http://link.aps.org/supplemental/10.1103/PhysRevLett.126.083001> for detailed explanation of the procedure for testing convergence of the calculations and tables of calculated state energies for Bi and Po.

[36] S. G. Porsev, U. I. Safronova, M. S. Safronova, P. O. Schmidt, A. I. Bondarev, M. G. Kozlov, I. I. Tupitsyn, and C. Cheung, *Phys. Rev. A* **102**, 012802 (2020).

[37] I. I. Tupitsyn, M. G. Kozlov, M. S. Safronova, V. M. Shabaev, and V. A. Dzuba, *Phys. Rev. Lett.* **117**, 253001 (2016).

[38] A. Kramida, Yu. Ralchenko, and J. Reader (the NIST ASD Team), *NIST Atomic Spectra Database (Version 5.7.1)* (National Institute of Standards and Technology, Gaithersburg, MD, 2019), <http://physics.nist.gov/asd>.

[39] G. G. Konan, L. Özdemir, and N. G. Atik, *J. Math. Fund. Sci.* **45**, 105 (2013).